CHAPTER VI

ELECTROCLINIC MEASUREMENTS - PART II: DETERMINATION OF THE COEFFICIENTS OF THE LANDAU THEORY

6.1 Introduction

In the previous chapter, we presented our measurements on the electroclinic response of some ferroelectric liquid crystals at a single frequency. We found that the electroclinic effect can be described using the Landau theory of the **A-C*** transition. In this chapter we describe experiments to estimate several coefficients of the Landau expansion. The procedure is similar to that used by Dupont et al. (1991). The main feature of this technique is to make both optical and current measurements in the **A*** phase of the ferroelectric samples. After giving a brief account of the earlier work, we give the theoretical background in the next section. In the subsequent sections we describe the experimental details and our results.

Glogarova el al. (1991) studied the influence of chirality on the electroclinic and dielectric properties of some mixtures. The chirality was changed by mixing the left-handed and right-handed varieties of the compound [L or D] 4-n-heptyloxybiphenyl-4'-(2-chloro-3-methy1)butanoate. They applied an **AC** field in the frequency range 120 Hz to 1.6 MHz, and measured the dielectric and electroclinic responses in the temperature range of T_{A-C*} to $T_{A-C*}+2K$ in order to determine its relaxation frequency τ^{-1}, the contribution to the dielectric susceptibility from the electroclinic

effect, viz., χ_{ec} and the electroclinic coefficient c of the soft mode. They found that $1/\chi_{ec}(T)$, $1/c(T)$ and τ^{-1} obey the Curie-Weiss law. From their analysis, they determined the first few coefficients of the Landau free energy and the viscosity of tlie soft mode. According to them, the c coefficient driving the linear interaction $cP\theta$ was the only one influenced by the chirality. It depended linearly on the concentration of the mixture and this dependence resulted in the shift of the phase transition temperature. When the chirality was lowered, there was a decrease in the dielectric susceptibility, electroclinic coefficient and the phase transition temperature.

Dupont et al. (1991) reported a study of the soft mode electroclinic coefficient as well as the current close to smectic A to smectic C* phase transition temperature under the same conditions of temperature, applied electric field and alignment in the chiral compounds, COS-C10 isoleucine, C_6 isoleucine and C7 valine. They measured both the tilt angle θ, and tlie induced polarisation $\mathcal{P}$ as functions of the applied field, at frequencies up to the MHz range, as well as the temperature T. They showed that the applied field had to be very low close to T_{A-C^*} to study the samples in tlie linear regime so that the tilt angle and induced polarisation were proportional to the field. They determined the first coefficients derived from the Landau expansion, viz., a, T_c^*, c and χ_P (where the symbols denote the physical quantities as mentioned in chapter V) together with the soft mode viscosity and relaxation frequency of the three compounds in the smectic A phase. χ_P was found to have a typical value of $\simeq 5$. Their value of $\epsilon_o \chi_P c$ had an order of magnitude of 100 which compared well with $\mathcal{P}/\theta$ ratios in the smectic C* phase. They obtained a $\approx 4\times10^4$ so that $A(T) \approx 10^6$ newton metre^{-2} far from the transition which is expected for this elastic constant. Their value of AT, $\approx$ 1 to 2K compared well with the difference in transition temperatures between the pure compounds and racemic rnixturcs. The

value of the relaxation frequency f_c obtained from the fit of the Lorentzian $\theta(\omega)$ ranged from 30 to 350 KHz 1 K above T_c. Their value of η determined from f_c tallied with the usual values of η for liquid crystals. They found that the simplest Landau theory of the transition worked well with only one temperature dependent coefficient $[A(T^*)]$, the other ones being constants within the temperature range of the smectic A phase.

As we mentioned in the previous chapter, even the chiral nematic phase above A* – N transition temperature exhibits a weak electroclinic effect. Zili Li *et al.* (1991) investigated the dynamics of the nematic electroclinic effect up to 100 KHz. They found that two relaxation processes acting cooperatively are involved near the transition temperature between the nematic and smectic A phases.

6.2 Theoretical background

As we have discussed in the previous chapter, the mean field expression for the free energy density of a smectic A liquid crystal made up of chiral molecules is given by

$$F = F_o + \frac{1}{2}A(T)\theta^2 + \frac{1}{2}\chi_{\mathcal{P}}^{-1}\mathcal{P}^2 - \mathcal{P}E - \frac{\epsilon_\infty E^2}{2} - c\mathcal{P}\theta \qquad (6.1)$$

Here F_o is the ground state free energy of the smectic A phase, $A(T)$ is the temperature dependent Landau coefficient given by $a(T - T_c)$, θ is the induced tilt angle, χ_P is the generalized susceptibility, $\mathcal{P}$ is the induced polarisation, E is the external field, c is the electroclinic coupling constant between $\mathcal{P}$ and θ, and ϵ_∞ is the high frequency dielectric constant.

Using the *linear* approximation (i.e., ignoring θ^4 term) and minimising the free

energy with respect to θ and $\mathcal{P}$, as was shown in the previous chapter, we get

$$\theta = \frac{\chi_{\mathcal{P}} c}{A(T^*)} E \tag{6.2}$$

and

$$\mathcal{P} = \chi_{\mathcal{P}} E + \frac{\chi_{\mathcal{P}}^2 c^2}{A(T^*)} E \tag{6.3}$$

where

$$\begin{aligned} A(T^*) &= a(T - T_c^*) \\ T_c^* &= T_c + \frac{\chi_{\mathcal{P}} c^2}{a} \end{aligned} \tag{6.4}$$

Due to the linear coupling $c\mathcal{P}\theta$, the transition temperature is displaced in a chiral compound compared to its non-chiral analogue. When a sinusoidal field $Ee^{i\omega t}$ is applied to the cell, $A(T^*)$ is to be replaced by $[A(T^*)] + i\omega q$, where η is the soft mode viscosity. Then we can expect the frequency dependences of the electroclinic tilt and of the electroclinic contribution to P to be Lorentzians with a relaxation frequency proportional to $\left[\tilde{a}\frac{(T-T_c^*)}{T_c^*}\right]$, where

$$\tilde{a} = aT_C^*. \tag{6.5}$$

Rewriting the phenomenological equation of motion [see equation (5.9)],

$$\eta\dot{\theta} + \tilde{a}\left(\frac{T - T_c^*}{T_c^*}\right)\theta = c\chi_{\mathcal{P}} E\ . \tag{6.6}$$

As $\mathrm{E} = E_o e^{i\omega t}$, correspondingly $\theta = \theta_o e^{i\omega t}$, i.e., $\dot{\theta} = i\omega\theta$.

Equation (6.6) can be written as

$$\eta(i\omega\theta) + \tilde{a}\left(\frac{T - T_c^*}{T_c^*}\right)\theta = c\chi_{\mathcal{P}} E$$

i.e.,

$$\theta = \frac{c\chi_{\mathcal{P}}E}{\tilde{a}\left(\frac{T-T_c^*}{T_c^*}\right)\left\{1+\frac{i\omega\eta}{\tilde{a}\frac{(T-T_c^*)}{T_c^*}}\right\}} - \frac{c\chi_{\mathcal{P}}E}{\tilde{a}\left(\frac{T-T_c^*}{T_c^*}\right)(1+i\omega\tau)} \quad \text{say,} \tag{6.7}$$

where

$$\tau = \frac{\eta}{\tilde{a}\left(\frac{T-T_c^*}{T_c^*}\right)} \tag{6.8}$$

is the relaxation time of the fluctuations of the order parameter θ. We now rewrite these equations in forms which will be useful to estirnate the coefficients of the Landau expression, following the procedure of Dupont et al. (1991). Equation (6.7) can be rewritten as

$$\theta = \frac{c\chi_{\mathcal{P}}E(1-i\omega\tau)}{\tilde{a}\left(\frac{T-T_c^*}{T_c^*}\right)(1+\omega^2\tau^2)} \tag{6.9}$$

from which the RMS value of θ

$$|\theta| = \frac{c\chi_{\mathcal{P}}E}{\tilde{a}\left(\frac{T-T_c^*}{T_c^*}\right)} \frac{1}{\sqrt{1+\omega^2\tau^2}} . \tag{6.10}$$

If the frequency is very low such that

$$\omega\tau \ll 1$$

we recover equation (6.2)

$$\theta \simeq \frac{c\chi_{\mathcal{P}}E}{\tilde{a}\left(\frac{T-T_c^*}{T_c^*}\right)} \tag{6.11}$$

$$\text{i.e.,} \quad e = \frac{\theta}{E} = \frac{c\chi_{\mathcal{P}}}{\tilde{a}\left(\frac{T-T_c^*}{T_c^*}\right)} \tag{6.12}$$

From equation (6.3) under a DC field,

$$\mathcal{P} = E\left[\chi_{\mathcal{P}} + \frac{c^2\chi_{\mathcal{P}}^2}{\tilde{a}\left(\frac{T-T_c^*}{T_c^*}\right)}\right] \tag{6.13}$$

When an AC field is applied,

$$\mathcal{P} = E\left[\chi_{\mathcal{P}} + \frac{c^2\chi_{\mathcal{P}}^2}{\tilde{a}\left(\frac{T-T_c^*}{T_c^*}\right)\{1+i\omega\tau\}}\right] \tag{6.14}$$

Again, if $\omega\tau \ll 1$, we recover equation (6.13).

In the SI system,

$$\begin{aligned} D &= \epsilon_o E + \mathcal{P} \\ &= \epsilon_o E + E\left[\chi_{\mathcal{P}} + \frac{c^2\chi_{\mathcal{P}}^2}{\tilde{a}\left(\frac{T-T_c^*}{T_c^*}\right)}\right] \end{aligned} \tag{6.15}$$

The dielectric permittivity of the medium along a direction perpendicular to the director is then given by

$$\epsilon_\perp = \frac{\mathrm{D}}{\mathrm{E}} = (\epsilon_o + \chi_{\mathcal{P}}) + \frac{c^2\chi_{\mathcal{P}}^2}{\tilde{a}\left(\frac{T-T_c^*}{T_c^*}\right)} \tag{6.16}$$

In the above equation, we have also to add the contribution from the very high frequency dielectric constant which arises from the polarisability due to the electron cloud. This contribution $\simeq \epsilon_o\chi_\infty$, where $\chi_\infty = n_o^2$. Here n_o is the ordinary refractive index.

From equations (6.12) and (6.16), by plotting $\epsilon_\perp$ vs. e, the y-intercept yields $(\epsilon_o + \epsilon_o\chi_\infty + \chi_{\mathcal{P}})$ and the slope gives $c\chi_P$.

6.3 Experimental set-up

We employed a set-up similar to the one described in the previous chapter, but with some modifications to measure the current passing through the cell. A block diagram of the experimental arrangemerit is shown in figure (6.1).

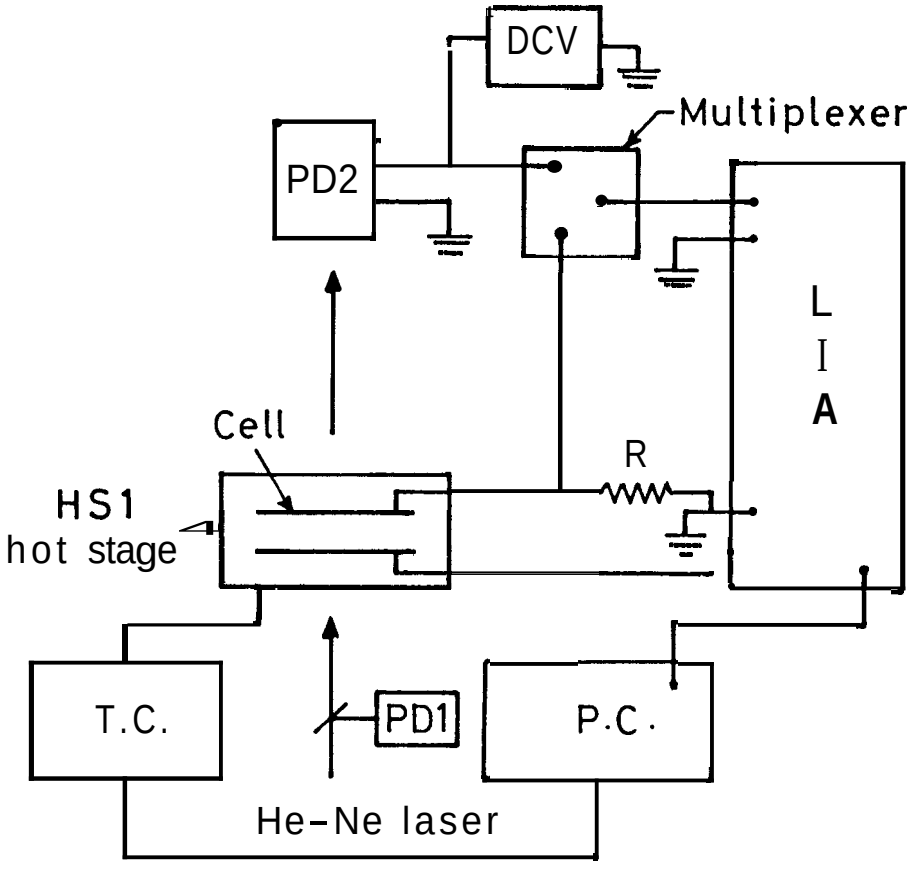

Figure 6.1. Block diagram of the experimental set-up used to measure the current and electrooptic response.

As described in the previous chapter, in the case of commercial compounds such as SCE-5, SCE-6 and the eighth, ninth, tenth homologues of the D-Series, i.e., [2S,3S]-4′-(2-chloro-3-methylpentanoyloxy)phenyl-*trans*-4″-n-alkoxy cinnamates, we got the homogeneous alignment of the sample relatively easily, by proper surface treatment of the cell walls and a slow cooling ($0.01°C/\text{min}$) of the sample from the isotropic phase. However, the seventh homologue (D7) of the D-series did not align by this method. So we had to adopt a slightly modified technique. We made a cell of thickness typically $\approx 8\ \mu m$ using ITO coated glass plates. The plates were pretreated with nylon dissolved in meta-cresol and methyl alcohol and rubbed unidirectionally. This cell was filled with the ferroelectric sample in the isotropic phase and was mounted in the cell holder, placed in the INSTEC HSI-i microscope hot stage. The temperature of the cell was regulated with the help of a P.C. (ZODIAC-2AT6). The temperature stability was around 10 mK. We cooled the sample slowly ($0.01°C/\text{min}$) to the C* phase, applied a DC electric field of 1 V and then slowly heated the sample at the same rate to the A phase, (2-3° above the C*-A transition temperature). By repeated slow cooling and slow heating of the sample across the A-C* transition temperature under a DC field, we could finally get a reasonably good homogeneous alignment. A standard resistance R=10 ohms was connected in series with the cell. A He-Ne laser was used as the light source. Using a glass plate as a partial reflector, the laser intensity was monitored using a photodiode (OSI-5K). The intensity of light transmitted through the cell was measured using a PIN photodiode (Hamamatsu 1722) which has a response time of $5nS$, the output of which was connected to a preamplifier which was built around the fast operational amplifier BB3551. The preamplified output is fed to a lock-in-amplifier (PAR5301) for optical signal measurement at the frequency of the applied field, and also to a DC multimeter (HP3457A) to measure the DC part of the signal. The lock-in-amplifier provided

both the field to be applied to the sample and also tlie phase-sensitive detection of the electrooptical signal from the photodiode. The electric current was also measured by using the lock-in-amplifier. In our initial manual measurements, we used a DPDT switch to change over between the optical and conductivity signals. This arrangement enabled us to measure both the signals under identical conditions of frequency, applied voltage and temperature of the sample. Later, we computerized the whole measuring system. Appropriate softwares were developed by one of our colleagues for this purpose, some working details of which will be given later. One of them was programmed to measure the required physical quantities as functions of temperature at a particular set frequency. The other software was programmed to measure the same physical quantities as functions of frequency at a particular temperature, then to step down according to specified temperature decrements and to make all the measurements as functions of frequency in the set temperature range. We replaced the DPDT switch in this case by a relay operated multiplexer as shown in the figure (6.1) to act as a switching device between the optical and conductivity signals.

The working sequence of the programmes which follows the manual operation closely is given below.

Program 1. The system waits for temperature stabilization and for tlie settling of tlie PAR 5301. It sets the sensitivity of the lock-in-amplifier for optimum measurement of the optical signal. It ensures that the optical signal is within the linear regime by decreasing or increasing the applied voltage appropriately. It records the optical signal and phase, the temperature of the hot stage is measured by the thermistor which also controls the given temperature, and temperature of tlie sample is measured by the platinum resistance thermometer (see Fig.5.4 of Chapter V). Then

the programme activates the multiplexer to change over to the conductivity channel, waits for the lock-in-amplifier to settle and measures the signal and phase. Then it switches back to the optical signal channel, measures the DC optical signal arid the reference laser intensity.

Then the programme lowers the terriperature by a preset value wliich depends on tlie optical response and makes all measurements as in the case of the previous value of the temperature. Provision is made in the programme for the stepping down of the temperature decrement according to the following scheme. The change in the optical rcsponsc between successive terriperature runs is stored. If the response changes between successive temperatures by a value greater than a *scaling factor* multiplied by the previous change, the temperature decrement is halved, otlicrwise it is unaltered. A scaling factor of 2 was found to be satisfactory in our set up. As we start tlie run at a ternperature about 2" to 3" above T_{A-C}• and approach T_{A-C}•, the optical signal rises steeply. The programme allows the readings to be taken at closer intervals of terriperature as T_{A-C}• is approaclied. A11 the values were stored in a file for further processing. the phase transition temperature is easily located as tlie slope of tlie optical signal versus temperature suddenly changes at that point.

program 2. The second programme is basically similar except that at each teniperature, tlie optical and current measurements are made at several presct frequencies in the range of 25 Hz - 100,000 Hz. The values of the optical and conductivity signals at a particular frequency and temperature are quite different. I-lence the program records the optical measurements as a function of set frequencies at a stretch. Using the multiplexer, the programme then switches over to the conductivity channel. It makes again all the measurements at tlie frequencies in the same order and at the same applied voltages as in the optical case.

6.4 Results and Discussion

We had to maintain the sample in the liquid crystalline phase till the completion of the experiment which took several days. But this non-stop heating resulted in a lowering of the transition temperatures due to a deterioration of the sample. In order to know the variation in transition temperatures, we frequently used tlic first programme to conduct the optical measurement and locate T_{A-C*}.

The liquid crystalline samples that we have used in our experiments had ionic impurities. They make a considerable contribution to the conductivity signal at low frequencies as the ions follow the field. But at higher frequencies ($\sim$ KHz) ions cannot follow the field and the contributions due to the capacitative coupling become prominent. This allows us to measure the electroclinic contribution to the dielectric constant which is needed in the analysis.

We measured the frequency dependence of the electroclinic $'f'$ signal starting from a few degrees above the A-C* transition temperature up to T_{AC*} for D7, D8, D9 and D10.

In figure 6.2, the ratio of the optical signal to applied voltage is plotted against frequency at various temperatures for the compound D7. As is to be expected tlie relaxation frequency increases with temperature. The data was fitted to a Lorentzian $\theta(\omega)$ (see equation 6.10) using a non-linear least squares fitting programme. The calculated variation is shown as a line in figures 6.3 for D7. The relaxation frequency τ^{-1} was obtained as a function of temperature using this procedure. The graph of $\frac{1}{\tau}$ vs. temperature is shown in figure 6.4 for D7. It shows that the relaxation frequency increases linearly with temperature in accordance with the prediction of the Landau theory (see equation 6.8). The electroclinic response to tlie dielectric

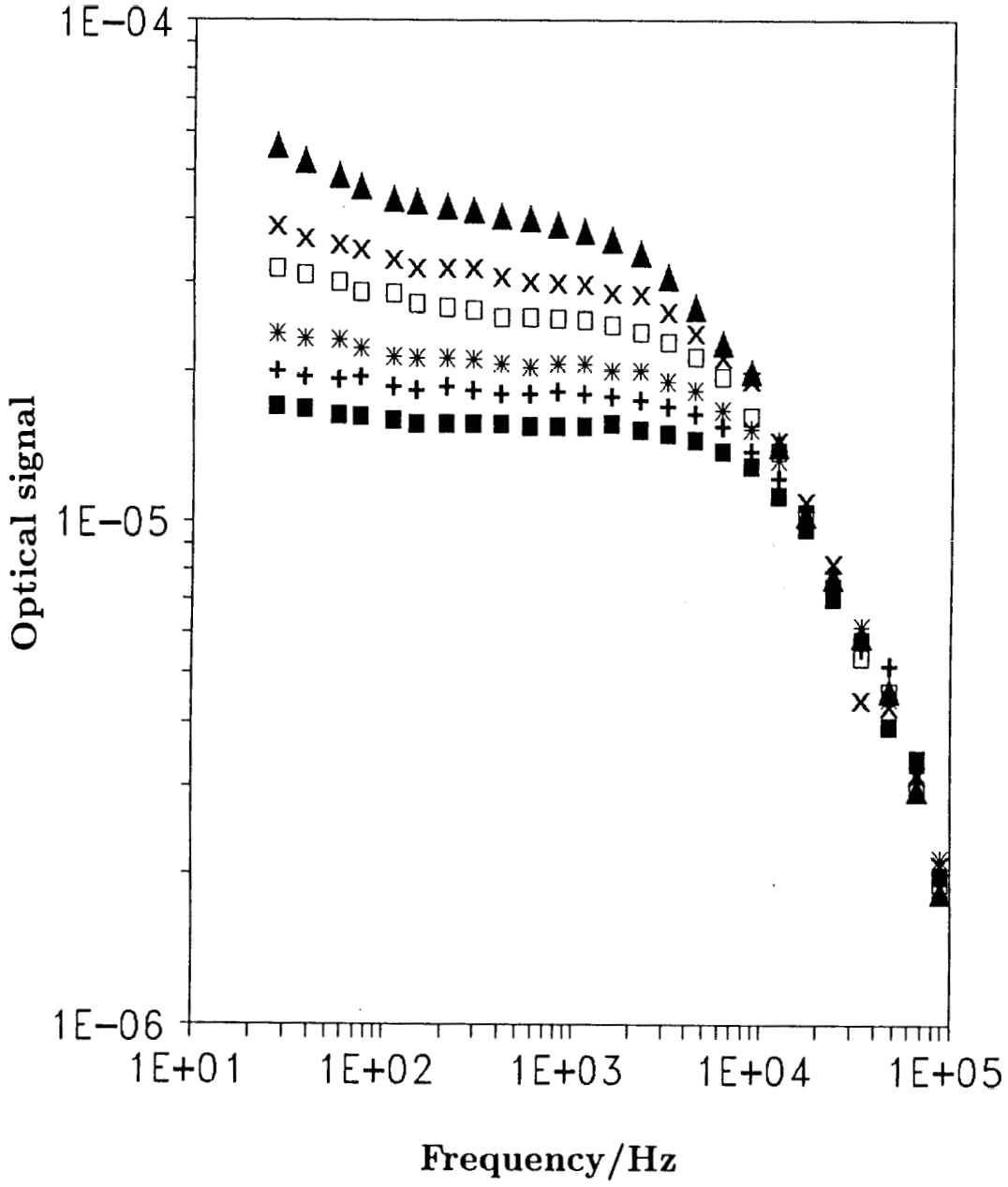

Figure 6.2. Variation of optical signal as a function of frequency at different temperatures in the smectic A phase of D7 with a thickness of 8.4 μm at (a) 330 K (A), (b) 330.2 K (x), (c) 330.4 K (□), (d) 330.6 K (*), (e) 330.8 K (+), (f) 331 K (■).

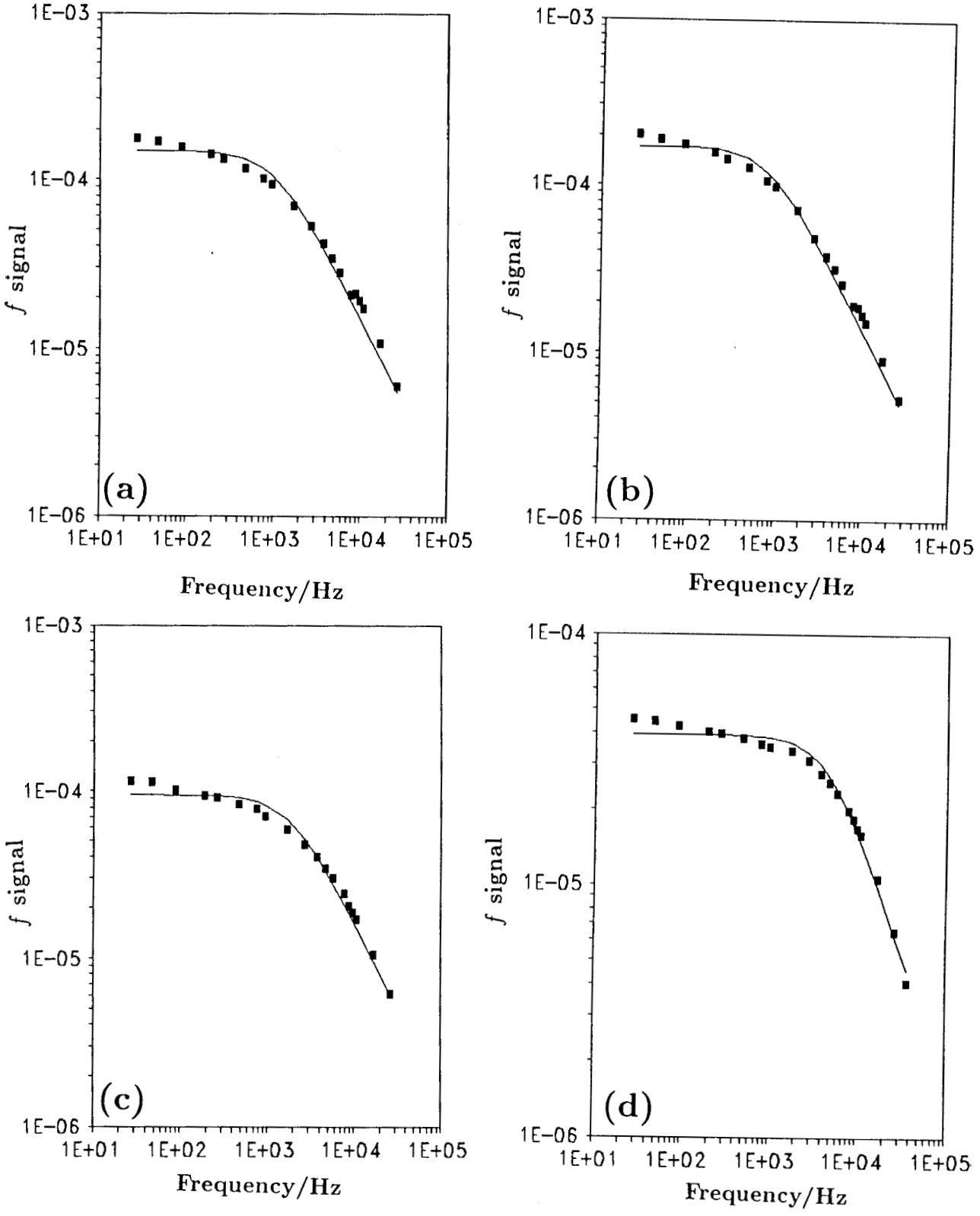

Figure 6.3. Variation of f signal as a function of frequency for the compound D7 at (a) 329.5 K, (b) 329.7 K, (c) 329.9 K and (d) 330.5 K.
Solid line gives the fitted Lorentzian.

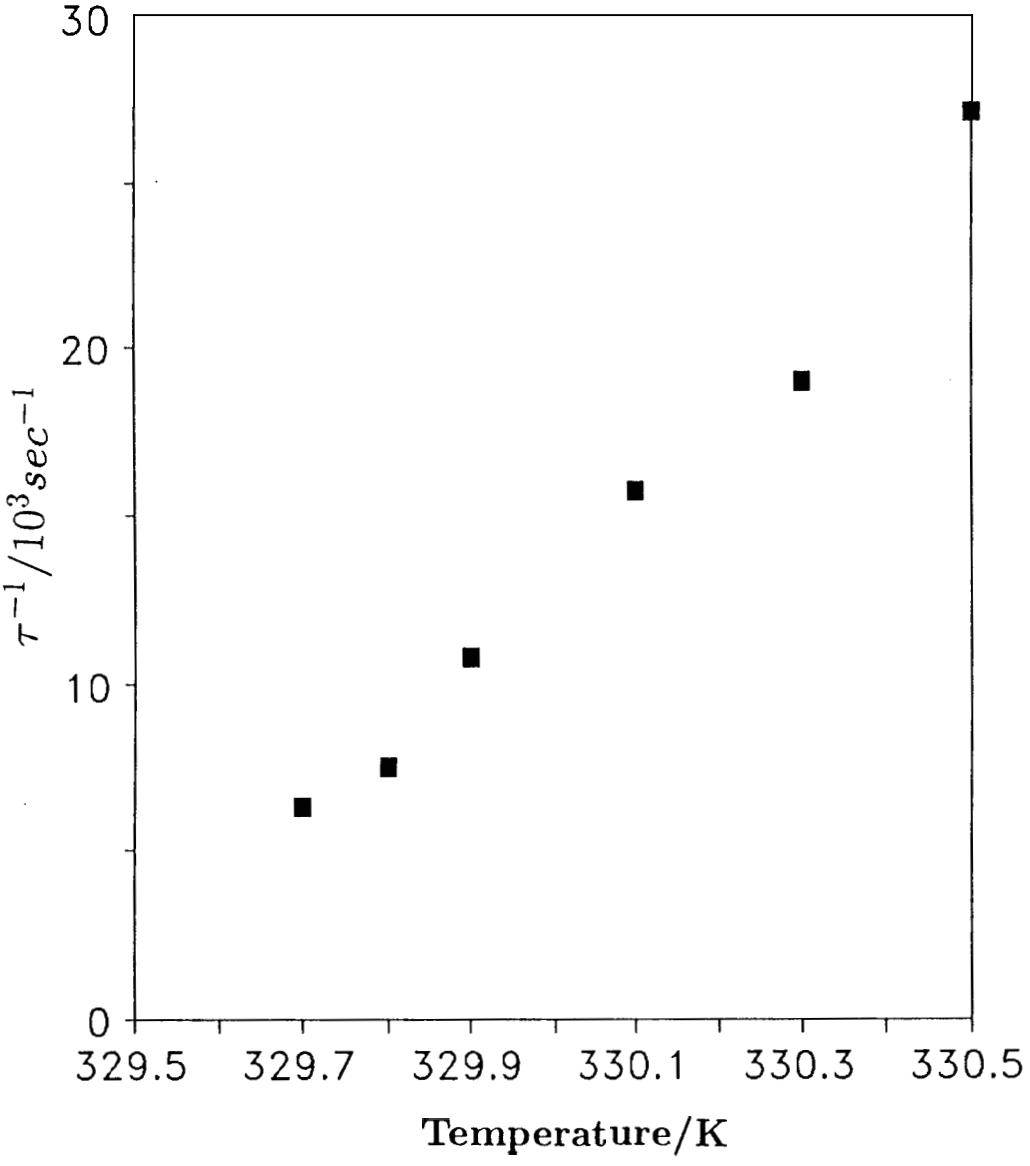

Figure 6.4. Variation of $1/\tau$ as a function of temperature for D7.

constant relaxes beyond that frequency.

Similar measurements have been made on D8, D9 and D10. Figures 6.5, 6.7 and 6.9 show the results of the fitted Lorentzians with the experimental data. Figures 6.6, 6.8 and 6.10 show that τ^{-1} varies linearly with temperature in all the cases.

The typical frequency dependence of the current (which is essentially capacitative) is shown in figure 6.11. It shows that there is a change of slope when tlie electroclinic cdntribution to the current relaxes.

In D9 and D10 wc have made dctailcd measurements of the current as a function of temperature at 1960 Hz and 5700 Hz respectively, simultaneously with the measurement of tlie optical signal.As the ionic impurities in the sample were quite high, we had to use relatively high frequency for measuring the current. We can use this data to estimate some coefficients of the Landau theory of the A-C* transition. We use the data in a temperature range in which these frequencies are below the relaxation frequency. Hence we can use equations (6.12 and 6.16) in further analysis of the data.

At these frequencies of measurement, we can assume that the ionic conductivity does not contribute significantly to the current and tlie cell acts like a capacitor. The capacitance of the cell is given by

$$C = \mid \frac{I}{\omega V} \mid = \epsilon_{\perp} C_o + C_{spacer}$$

where $\epsilon_{\perp}$ is the dielectric permittivity of the medium along a direction perpendicular to the director, C_o is the capacitance of the part of the empty cell, without tlie spacer which was calculated by the geometrical parameters of the cell. C_{spacer} is the capacitance of tlie part of tlie cell which had mylar spacers which was also calculated by the geometrical parameters.

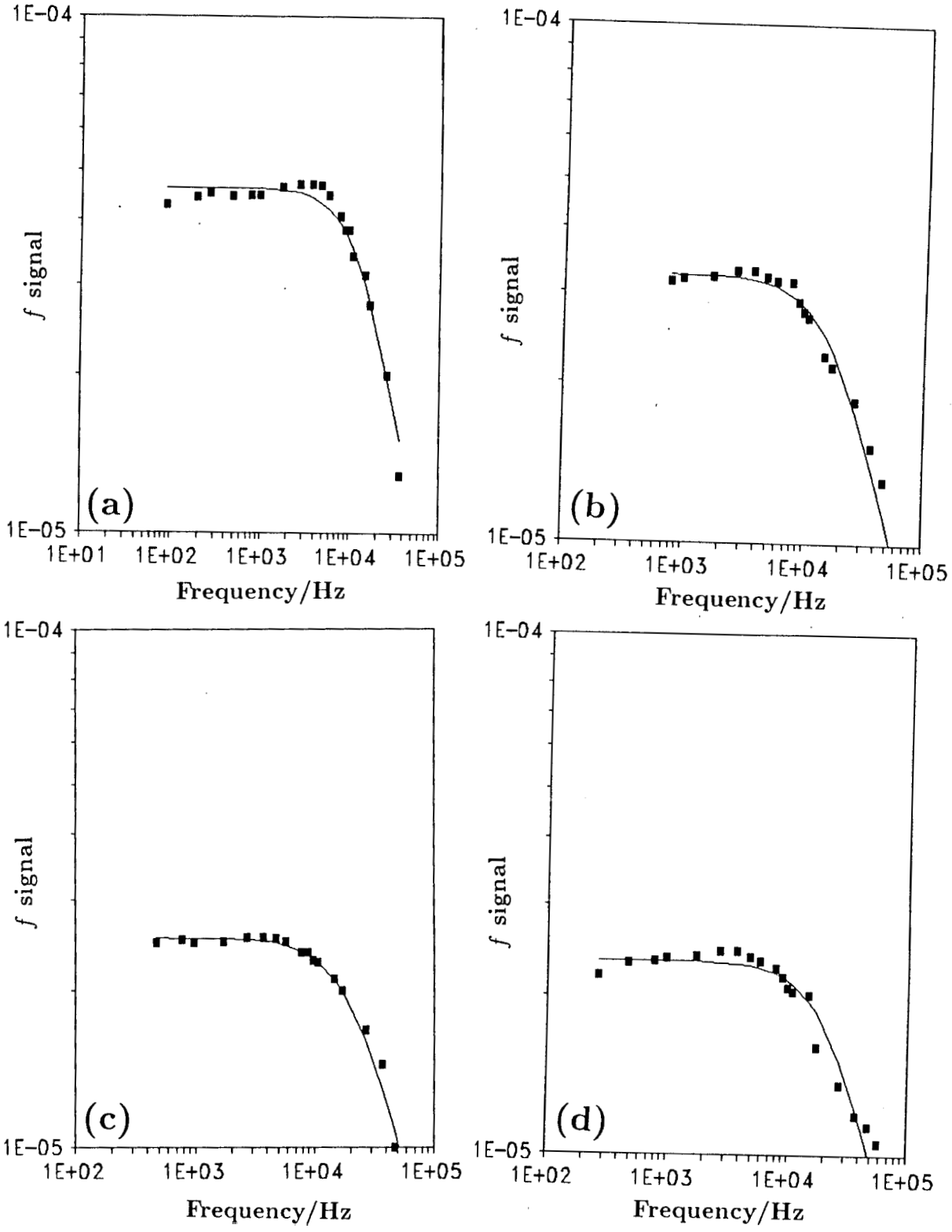

Figure 6.5. Variation of f signal as a function of frequency for the compound D8 at (a) 341.3 K. (b) 341.7 K, (c) 341.9 K and (d) 342 K.

Solid line gives the fitted Lorentzian.

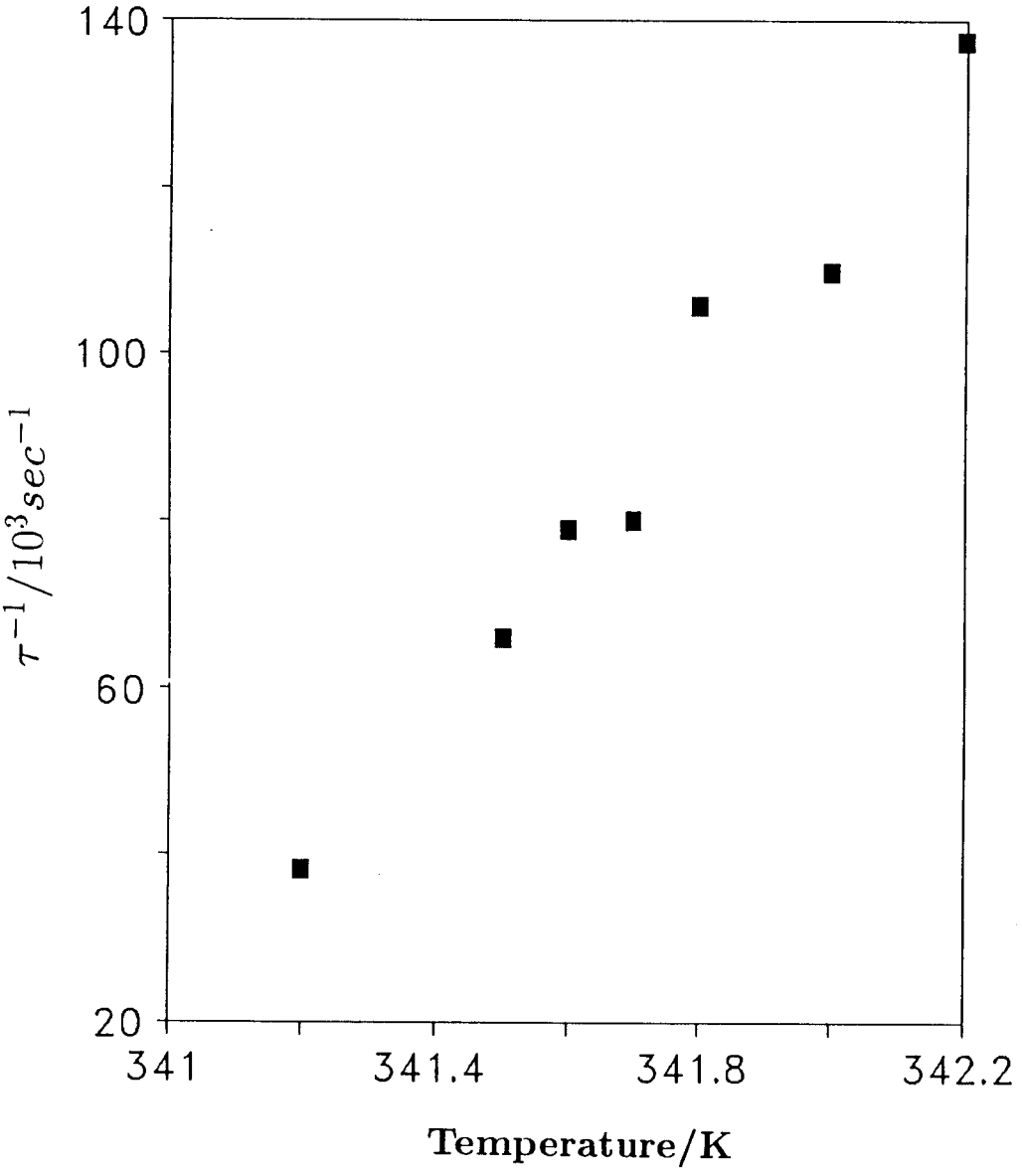

Figure 6.6. Variation of $1/\tau$ as a function of temperature for D8.

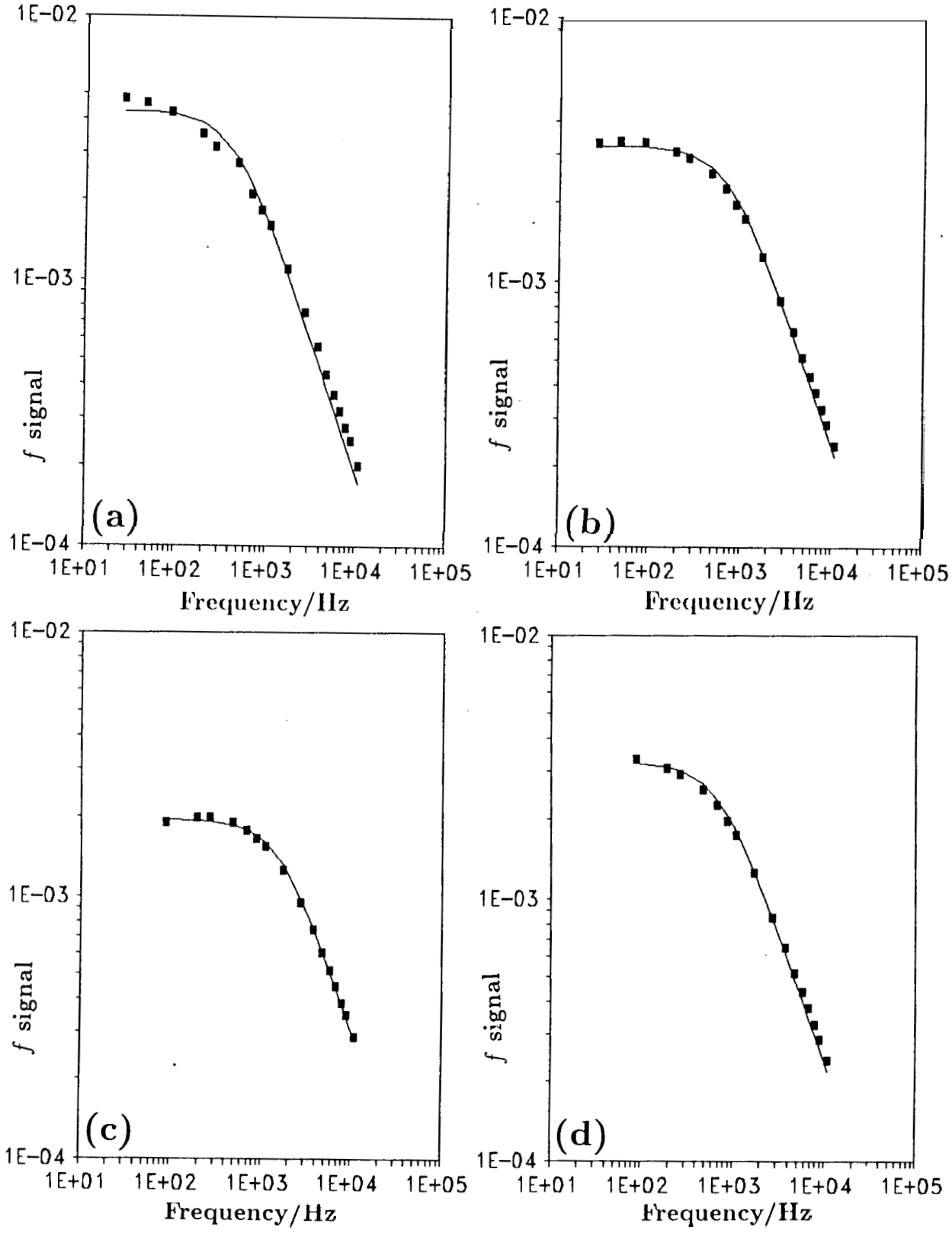

Figure 6.7. Variation of f signal as a function of frequency for the compound D9 . (a) . K, (b) . K, (c) 339.7 K and (d) 340.1 K.

Solid line gives the fitted Lorentzian.

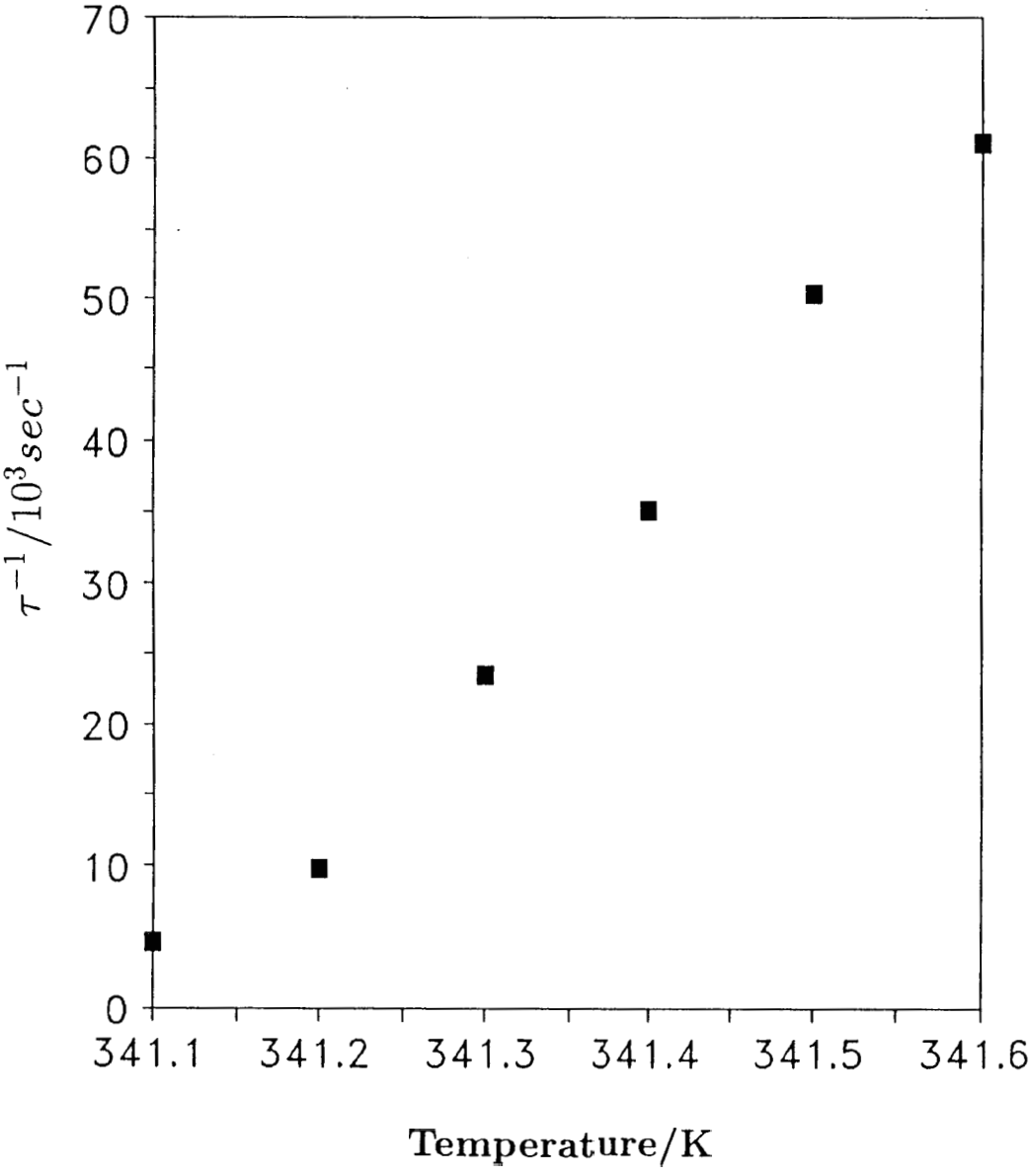

Figure **6.8.** Variation of $1/\tau$ as a function of temperature for D9.

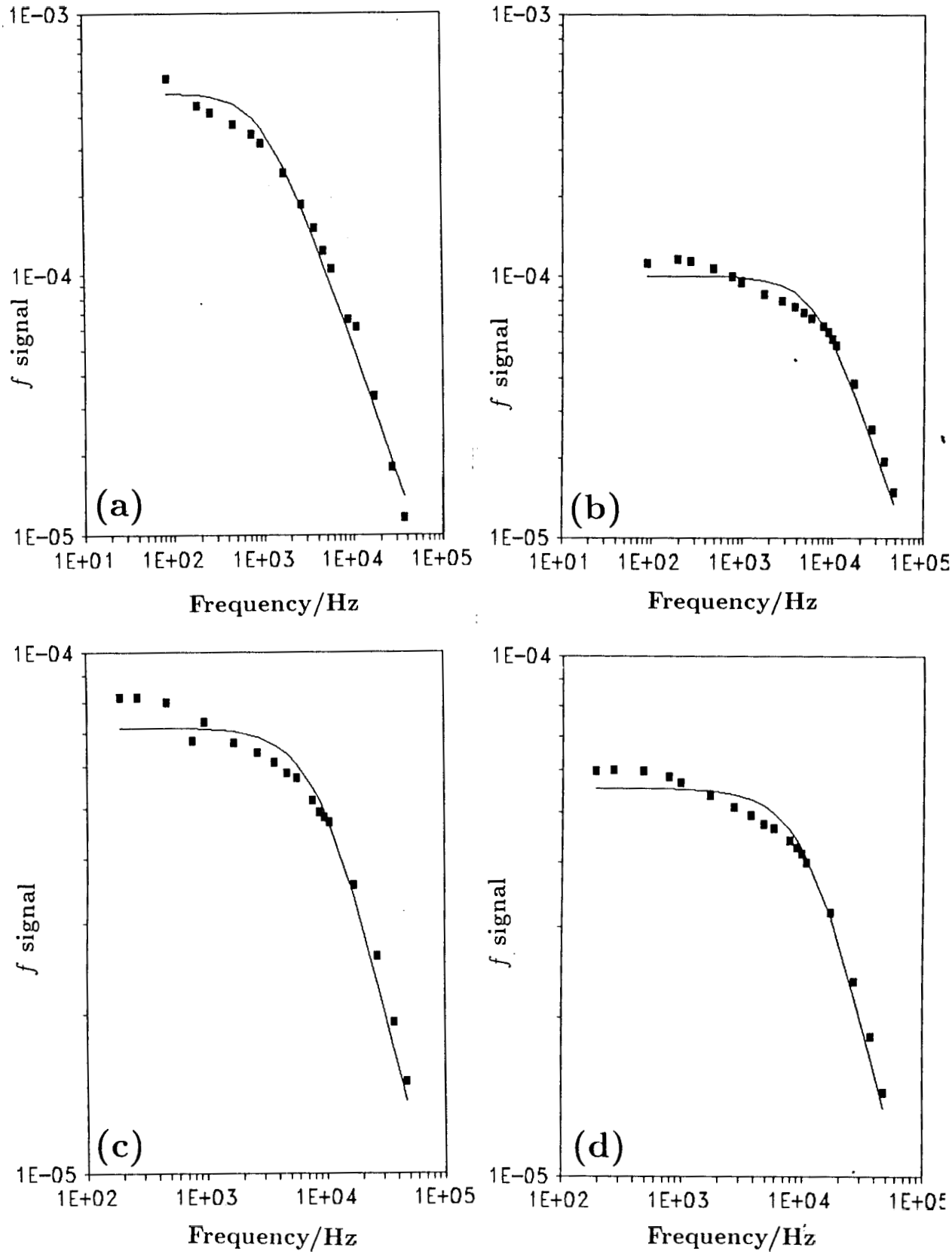

Figure 6.9. Variation of f signal as a function of frequency for the compound D10 at (a) 347.9 K, (b) **348.5** K, (c) 348.7 K and (d) 348.9 K. Solid line gives the fitted Lorentzian.

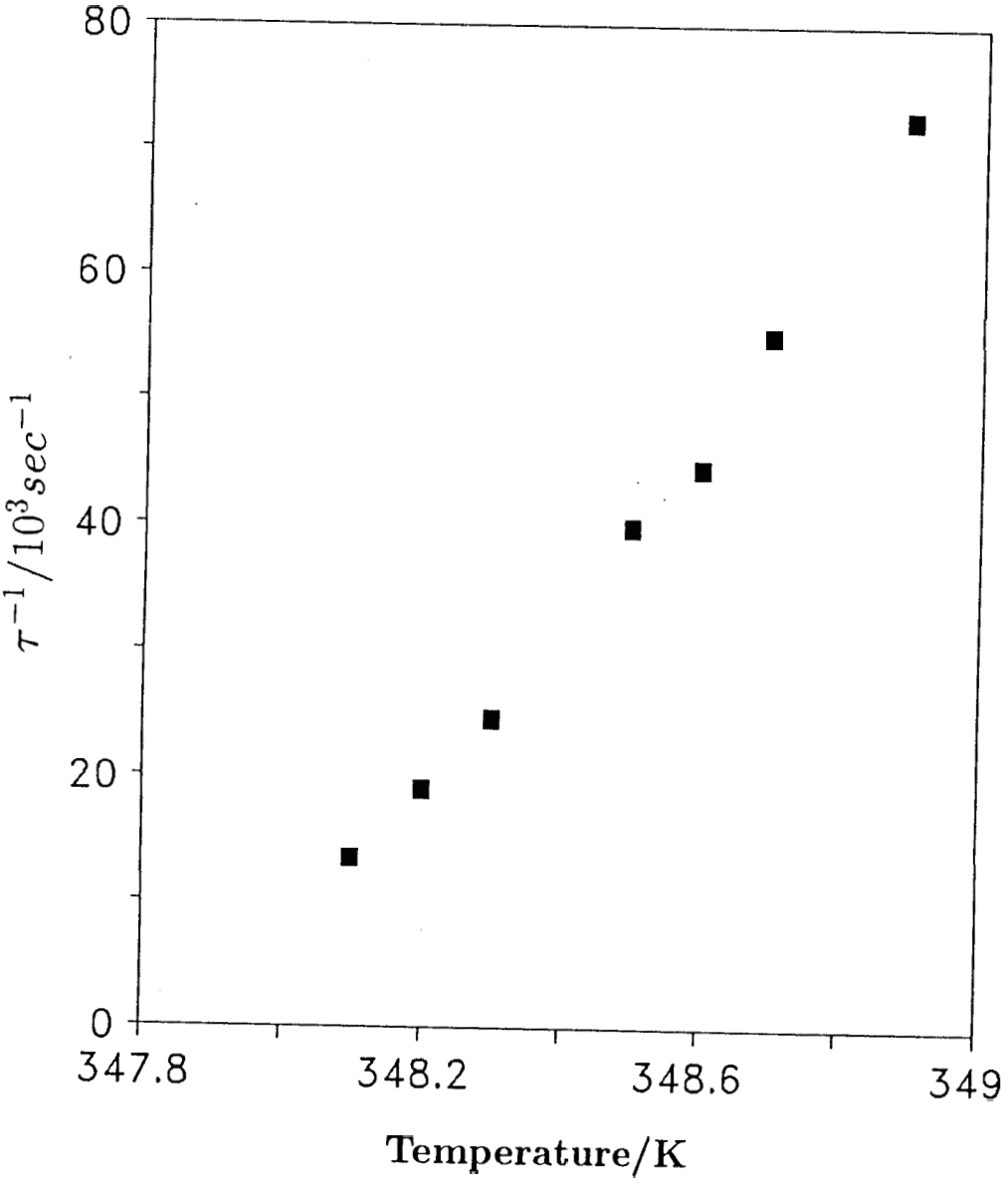

Figure 6.10. Plot of $1/\tau$ vs. temperature for D10.

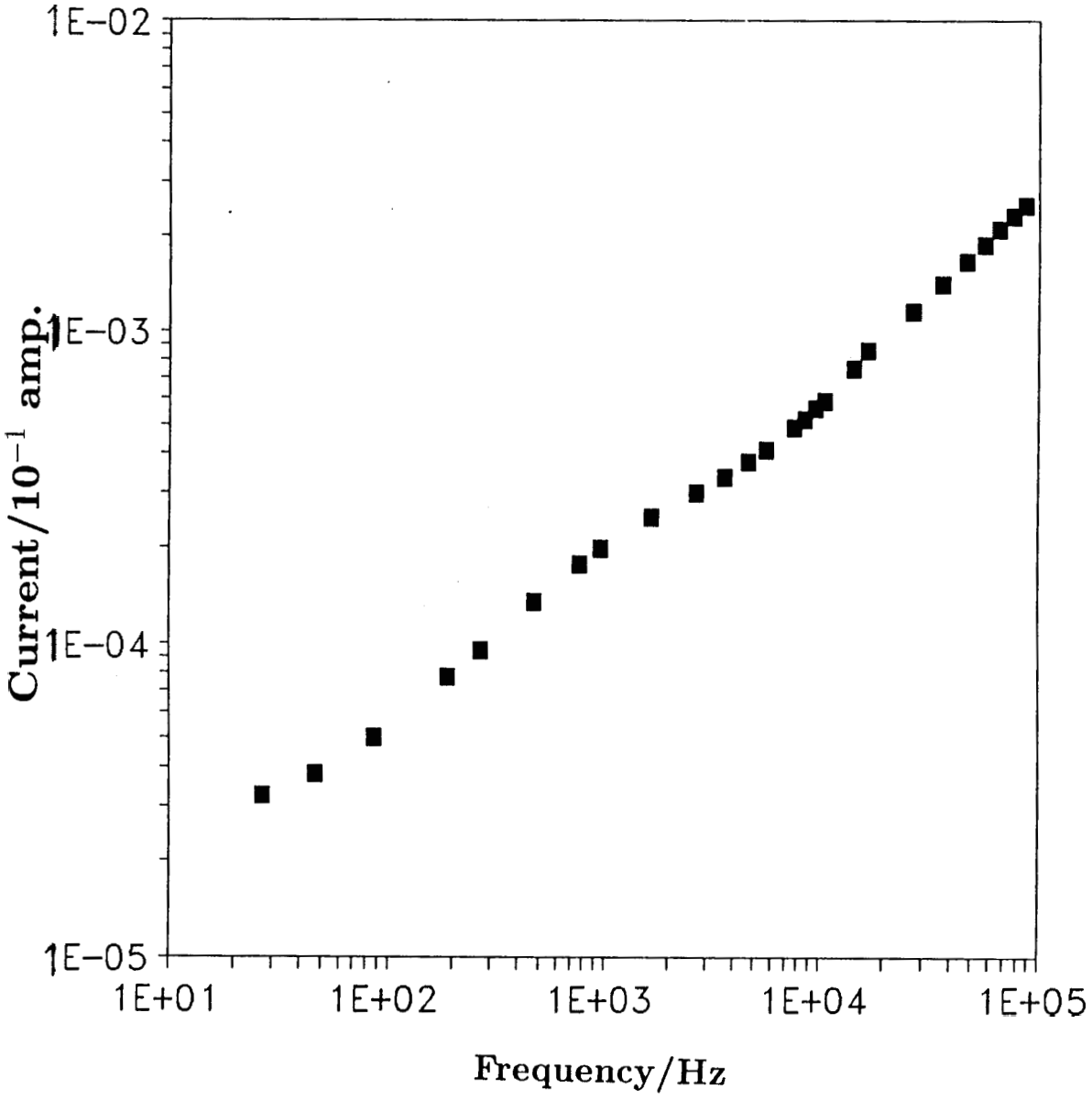

Figure 6.11. Frequency dependence of the current through the cell for the compound D9 at 342 K.

The above equation can be rewritten as

$$\frac{C}{C_o} = \frac{C_{spacer}}{C_o} + \epsilon_\perp \tag{6.17}$$

C_{spacer}/C_o was subtracted from the value of C/C_o to get the actual value of $\epsilon_\perp$. We plotted $\epsilon_\perp/\epsilon_o$ versus e $= (\theta/E)$ at various temperatures. Figure 6.12 shows this variation for D9 and figure 6.13 for D10.

As expected from equations (6.12) and (6.16) the variation of $\epsilon_\perp$ vs. e is a straight line within the accuracy of our measurements. As discussed after equation (6.16) the Y-intercept yields $(1+\chi_\infty+\chi_{\mathcal{P}}/\epsilon_o)$ and the slope gives $c\chi_{\mathcal{P}}$. $\chi_\infty = n_o^2$, where n_o is the ordinary index $\simeq 1.6$. Hence from the Y-intercept we can calculate $\chi_{\mathcal{P}}$ and using this value tlie coupling coefficient c can be calculated from the slope. From the graph of e^{-1} vs. T, using equation (6.12), the corresponding slope gives $\tilde{a}$. In tlie case of D9 and D10, from figures 5.14 and 5.15, the slopes have the rnagnitudes 2.1×10^7 and 1.6×10^7. Hence we could calculate $\tilde{a}$ for D9 and D10.

Using equation (6.8), substituting the value of $\tilde{a}$, the viscosity coefficient η can be calculated. We have shown all tlie calculated values in table 6.1.

The values given in table 6.1 broadly agree with the expected values. If we corn-pare these values with those of Dupont et al. (1991) for example, the corresponding values seem to be of the same order. Our values of $\chi_{\mathcal{P}}/\epsilon_o$ for D9 and D10 are somewhat larger than the values got by Dupont et al. for their compounds. This may partly be due to the presence of an additional COO group in the molecular structure of the compounds that we have used. This will enhance the lateral dipole moment of the molecule. The values of c, a, AT, in our measurements are of tlie same order as in their compounds. The viscosity coefficient η is 0.01 Ns/m^2 which is of the right order for liquid crystals at high temperatures. These numbers are

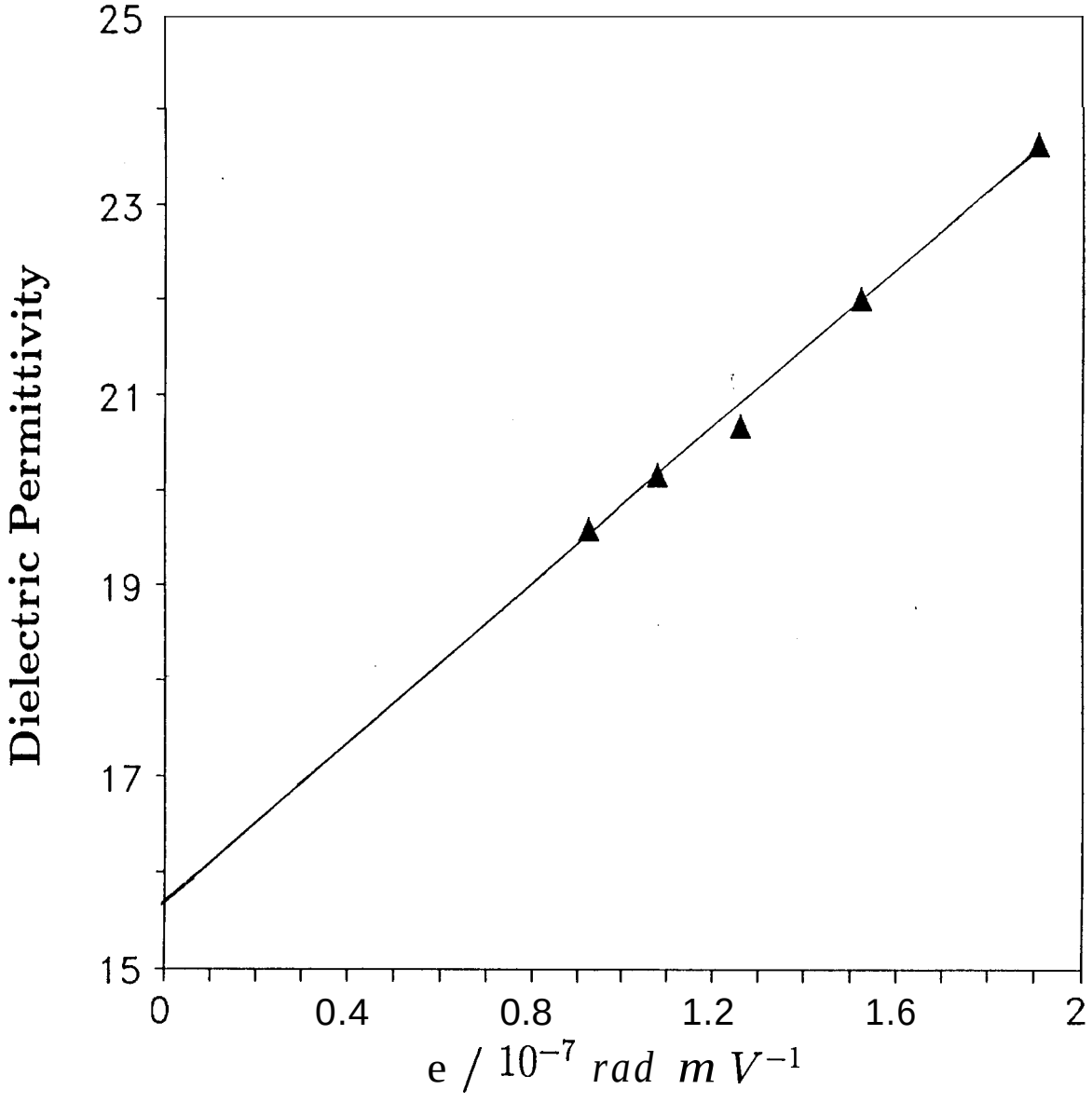

Figure 6.12. Dielectric permittivity as a function of the EC coefficient for the compound D9.

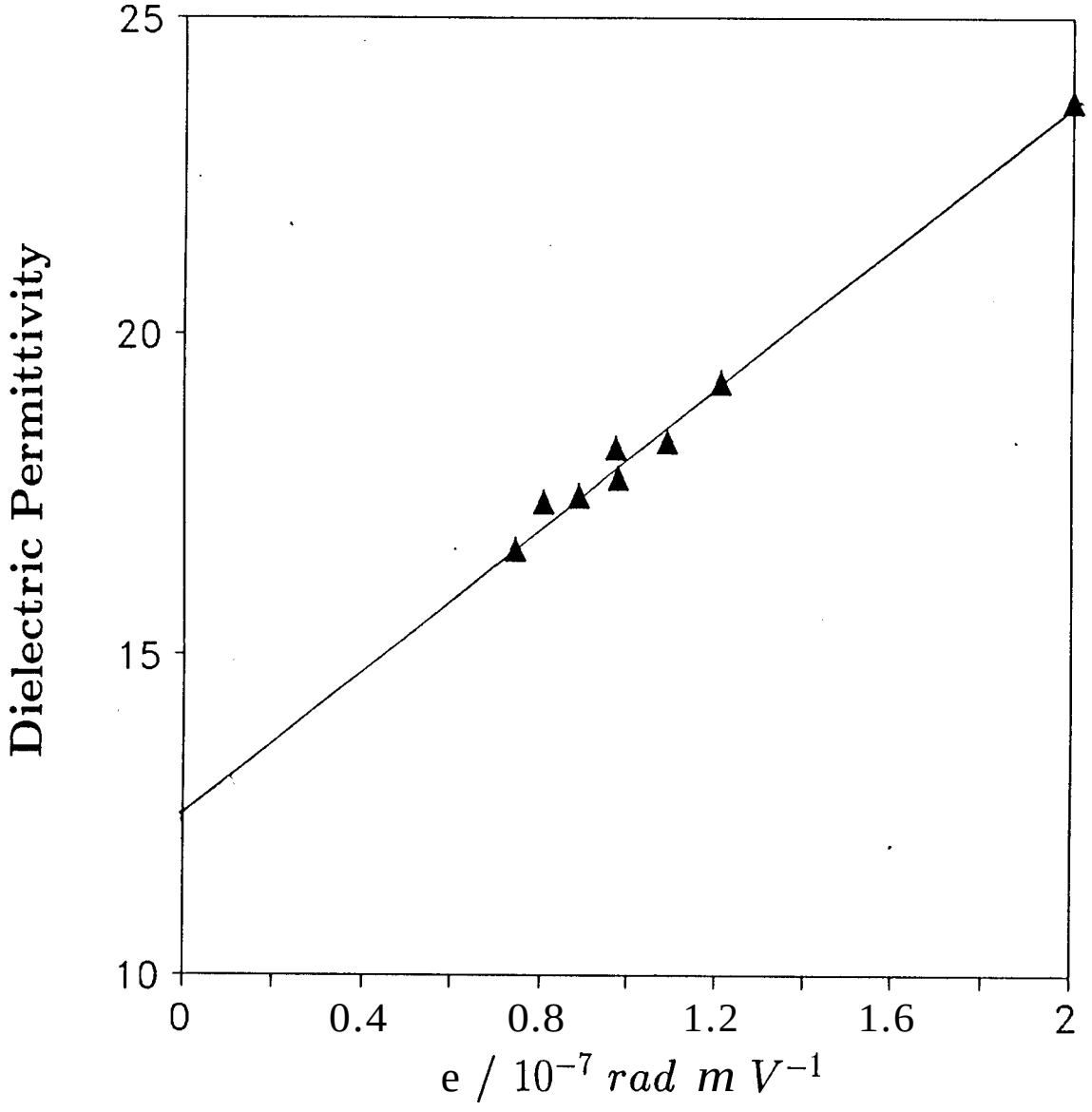

Figure 6.13. Dielectric permittivity as a function of the EC coefficient for the compound D10.

Table 6.1

Coefficients of the Landau theory

Coefficients	Compound	
	D9	D10
$\chi_{\mathcal{P}}/\epsilon_o$	11.6	8.5
$\chi_{\mathcal{P}}c(Cm^{-2}rad^{-1})$	3.73×10^{-4}	4.87×10^{-4}
$c(NC^{-1}rad^{-1})$	0.36×10^{7}	0.65×10^{7}
$a(Nm^{-2} \times K^{-1})$	0.78×10^{4}	0.78×10^{4}
$\Delta T_c(K)$	1.7	0.4
$\eta\ (Nsm^{-2})$	0.01	0.01

also consistent with the fitting parameters obtained on D8 in the previous chapter, where we analysed only the optical data in terms of the Garoff-Meyer model. However, we should note that in the present analysis η is assumed to be temperature independant.

Thus the dynamic measurements on the *soft mode* electroclinic effect in the **A*** phase can be used to estimate all the parameters of the *linearised* Landau model of the A-C* transition.

References

DUPONT,L., GLOGAROVA,M., MARCEROU,J.P., NGUYEN,H.T., DESTRADE,C. and LEJCEK,L., 1991, J. Phys. *II,* France, 1, 831.

GLOGAROVA,M., DESTRADE,Ch. and MARCEROU,J.P., BONVENT,J.J., NGUYEN H.T., 1991, Ferroelectrics, 121, 285.

ZILI LI, AMBIGAPATHY,R., PETSCHEK,R.G. and ROSENBLATT,C., 1991, *Phys.* ***Rev.*** A, 43, 7109.